

Moisturizing emulsion systems based on the novel long-chain alkyl polyglucoside emulsifier

The contribution of thermoanalytical methods to the formulation development

Milica Lukic · Ivana Pantelic · Rolf Daniels ·
Christel Müller-Goymann · Miroslav Savic ·
Snezana Savic

Received: 23 November 2011 / Accepted: 20 January 2012 / Published online: 19 February 2012
© Akadémiai Kiadó, Budapest, Hungary 2012

Abstract Mesomorphic behavior of the novel long-chain alkyl polyglucoside emulsifier comprising arachidyl alcohol (C_{20}), behenyl alcohol (C_{22}), and arachidyl glucoside was investigated in order to determine the prevalent stabilization mechanism and moisturizing capacity of emulsion systems based on it. For this to be accomplished thermoanalytical methods (differential scanning calorimetry and thermogravimetric analysis) coupled with microscopy, rheological, X-ray diffraction methods and a short-term in vivo study of skin hydration level were performed. Obtained results have proved that C_{20}/C_{22} alkyl polyglucoside mixed emulsifier is able to provide the synergism between the two main types of lamellar phases, the liquid-crystalline ($L\alpha$), and the gel crystalline ($L\beta$) one, building the emulsion systems of different stability and performance. Formation of lamellar structures influenced for more than one half of water within the system to be entrapped. Conducted investigation of

hydration potential in real-time conditions provided valuable information on the investigated emulsion vehicles' moisturizing potential as well as their contribution to the skin barrier improvement. Therefore, it could be expected that emulsions based on this alkyl polyglucoside emulsifier could influence the delivery of active ingredients of both the lipophilic and hydrophilic type. The employment of thermoanalytical methods in our work suggests the possibility for thermal methods to be used more frequently in the characterization of both the novel raw materials and the belonging emulsion systems.

Keywords Alkyl polyglucoside emulsifier ·
Moisturizing capacity · Emulsions · Thermal methods

Introduction

Despite the fact that nowadays the attention of scientific community engaged in the development of topically applied preparations is focused on new carriers like nano-sized lipid carriers, conventional emulsion systems remain an interesting field of research. For the most part, this is a result of the constant exploration of novel raw materials used in emulsion development and in this field alkyl polyglucoside (APG) surfactants represent a very interesting group.

For the last 10 years the growing interest concerning APGs, the so-called sugar surfactants, over standard, traditionally used polyoxyethylene derivatives, is mainly because of their advantages with regard to skin and environment compatibility [1, 2]. APGs are mostly obtained from renewable raw materials and, in the most situations, are found to be non-toxic and -allergic [3–5]. These sugar-based emulsifiers are in the form of mixed emulsifiers

M. Lukic (✉) · I. Pantelic · S. Savic
Department of Pharmaceutical Technology and Cosmetology,
University of Belgrade-Faculty of Pharmacy,
Vojvode Stepe 450, Belgrade, Serbia
e-mail: mlukic@pharmacy.bg.ac.rs

R. Daniels
Department of Pharmaceutical Technology, Eberhard-Karls
Universität Tübingen, Auf der Morgenstelle 8, Tübingen,
Germany

C. Müller-Goymann
Department of Pharmaceutical Technology, Technische
Universität Braunschweig, Mendelssohnstr. 1,
38106 Braunschweig, Germany

M. Savic
Department of Pharmacology, University of Belgrade-Faculty of
Pharmacy, Vojvode Stepe 450, Belgrade, Serbia

(emulsifying waxes). They consist of alkyl glucoside and at least one fatty alcohol and their head sugar unit contains a number of free hydroxyl groups. They enable complex water binding which could provide additional skin moisturization, thus having an impact on skin permeability and penetration potential of drugs and cosmetics [6].

The skin compatibility of sugar-based emulsion vehicles is mostly the consequence of their special skin-similarity structure. Although stratum corneum (SC) is commonly presented as a brick-and-mortar structure, the corneocytes within the SC are in fact embedded in lipid lamellar structures [7]. Hence, it was shown that APG-based vehicles mimic SC organization well as the result of lyotropic liquid crystals formation [8, 9]. Liquid crystals are known to have a highly ordered microstructure and are further capable of forming multilamellar structures, which can act as a specific modulator for water retention in the SC. Depending on the colloidal structure the vehicle may affect the skin moisture content by controlling the mode of water distribution within the system. In this context, the mesomorphic behavior of alkyl polyglucoside emulsifiers can be responsible for different modes of water incorporation [10].

Thermolanalytical methods—thermogravimetric analysis (TG) and differential scanning calorimetry (DSC) have already found their use in the research of various dispersed systems. Mass transfer phenomena during solidification and melting within an emulsion submitted to steady cooling and/or heating can be used for obtaining diverse information—stability concerns as well as physicochemical characterization of emulsions [11–13]. However, DSC is ideally suited when phase transition phenomena are investigated and therefore this method is employed in the study of different lipids and their mixtures with water and surfactants [14–17]. According to these statements, it is expected that DSC technique could provide valuable information concerning emulsion systems stabilized with APG emulsifiers, particularly those combined with long-chain fatty alcohols. On the other hand, thermogravimetric analysis can be used for water binding mechanism investigation and further structural analysis [18, 19]. Concerning the conventional emulsion vehicles, the mode of water distribution is of special interest since the bulk (free) water evaporates shortly after their application, while interlamellar (fixed) water needs certain time to be liberated from the system [20]. Therefore, TG could contribute to the investigation of mesomorphic behavior of APG emulsifiers and evaluation of moisturizing capacity of the APG-based emulsion vehicles.

In this study, a long-chain APG emulsifier comprising arachidyl alcohol (C_{20}), behenyl alcohol (C_{22}), and arachidyl (C_{20}) glucoside was investigated regarding its potential to create lamellar mesophases. It was of interest to evaluate this cosmetic raw material as a stabilizer of emulsion systems with prospective capability to hold “depot” water for a prolonged skin moisturization (skin hydration effect). Therefore, in order to characterize the inherent structure and mode of water distribution within its selected binary and ternary systems differing in oil phase two thermoanalytical methods were conducted. In addition, the results obtained were correlated to other techniques commonly employed for these systems such as microscopy, rheological, and X-ray diffraction methods. In parallel, a short-term in vivo study of their skin hydration potential was performed.

Experimental

Materials

Investigated emulsifier, Arachidyl alcohol, behenyl alcohol, and arachidyl glucoside (Montanov[®] 202, kindly provided by Seppic, France) was used for all binary and ternary systems preparation (Tables 1, 2). Binary systems were prepared with emulsifier/water ratios (emulsifier wt%): 1:12.33 (7.5%), 1:7.7 (11.5%), 1:5.67 (15%), 1:4 (20%), 1:2.33 (30%), 1:1.5 (40%) and labeled B1, B2, B3, B4, B5, and B6, respectively (Table 1). Ternary systems with fixed emulsifier/water ratio (1:7.7) and increasing percentage of oil phase (5, 10, 20, and 30 wt% of medium-chain triglycerides) were prepared and labeled T5mc, T10mc, T20mc, and T30mc, alongside with two samples with the same emulsifier/water ratio and 20 wt% of different oil phases: avocado oil and liquid paraffin oil labeled T20ao and T20lp, respectively (Table 2). Water phase for all samples was double distilled water and 0.5% Euxyl[®] K 300 (Schülke & Mayr, Germany) was used for preservation.

Methods

Preparation of samples

Binary systems were prepared by heating the preserved water and emulsifier in sealed glass vials to 80 °C, stirred at constant temperature for 1 min (1,000 rpm) and then for

Table 1 Composition of binary systems

Sample	B1	B2	B3	B4	B5	B6
Arachidyl alcohol, behenyl alcohol, arachidyl glucoside	7.5	11.5	15	20	30	40
Purified water	92.5	88.5	85	80	70	60

Table 2 Composition of ternary systems

Sample	T5 mc	T10 mc	T20 mc	T30 mc	T20 ao	T20 lp
Arachidyl alcohol, behenyl alcohol, arachidyl glucoside	10.92	10.23	9.19	8.05	9.19	9.19
Medium-chain triglycerides	5	10	20	30		
Avocado oil					20	
Liquid paraffin						20
Purified water	84.08	79.77	70.81	61.95	70.81	70.81

3 min at 500 rpm. The samples were removed from the heating plate but the mixing was continued at 400 rpm to the room temperature. For the preparation of ternary systems the oil phase heated to the same temperature (80 °C) was added to water/emulsifier mixture and the same mixing procedure was conducted.

Polarization microscopy

Colloidal structure of the samples was observed by a Carl Zeiss ApoTome Imager Z1 microscope (Zeiss, Germany) integrated with digital AxioCam ICc1 camera and Axio-Vision 4.6 computer software. A pin-tip amount of each sample was smeared on the microscope glass slide, covered with the cover slip, and pressed to make it as thin as possible. 200× and 400× magnifications were captured with cross polarizer in bright field using wavelength (λ) plate, to detect birefringence.

Small-angle X-ray diffraction (SAXD)

To provide an insight to the possible presence of the liquid-crystalline phases within the systems, SAXD measurements were performed using a position-sensitive detector (Braun, Munich, Germany) for all investigated samples. The semisolids were pressed between Capton foils (Krempel, Voihingen, Germany) to a thickness of 1 mm, avoiding air bubbles. X-rays were produced by a PW-1730 generator (Philips, Kassel, Germany) with a copper anode (current 25 mA, k 0.154 nm, accelerating voltage 40 kV). The exposure time was 300 s at ambient temperature. From diffraction angle theta (θ) the interlayer spacings were calculated according to the Bragg's law.

Wide-angle X-ray diffraction (WAXD)

To obtain full structural information on the samples, short-range ordering was examined using WAXD measurements. Diffraction patterns were collected using an X-ray goniometer PW-1050/25 (Philips, Germany), coupled with a Xe-filled linear counter (Fuji, Japan). X-rays were produced by an X-ray generator PW-1730 (Philips, Germany)

using a copper anode (anode current 25 mA; k 0.154 nm, accelerating voltage 40 kV). From diffraction angle theta (θ), the intermolecular distances were calculated according to the Bragg's law.

Thermoanalytical measurements

Differential scanning calorimetry (DSC)

DSC measurements were performed in order to assess phase transition phenomena in all prepared samples and to obtain an information about mesomorphic behavior and stabilization mechanisms providing by investigated APG emulsifier. Small amount of samples (between 10 and 12 mg) was accurately balanced (XP205 DeltaRange[®] analytical balance, Mettler Toledo, Germany) in aluminium pans, hermetically sealed and analysed with Mettler DSC 820 (Mettler Toledo, Germany). As a reference an empty pan was used. Samples were heated from ambient temperature (25 °C) to 120 °C, with the heating rate of 2 K/min to compare endothermic transition enthalpies of test and reference samples. Duplicate measurements, at least, were performed for all samples.

Thermogravimetric analysis (TG)

TG was performed in order to assess the mode of water distribution in investigated samples, implying the complexity of their colloidal structure. Small amount of samples were placed in open aluminium pans and heated in Netzsch STA 409PG (Netzsch, Germany), from 30 to 110 °C with isothermal segments at the beginning and ending of each measurement. The heating rate was set at 5 K/min. All samples were analysed in duplicate.

Rheological measurements

Continual rheological measurements were performed for both binary and ternary samples after 7 days storage at room temperature (Rheometer Rheolab MC 120, Paar Physica, Germany). All measurements were carried out using cone/plate measuring system (diameter 50 mm, angle

1°), with 0.05 mm sample thickness, at 20 ± 0.1 °C (in triplicate). During continual testing controlled shear rate procedure was applied (shear rate 0–200 s⁻¹ and back again to the start point, each stage lasting 120 s).

Viscoelastic behavior of the ternary systems was studied using dynamic (oscillatory) measurements. Oscillatory measurements were conducted using cone/plate measuring system (diameter 75 mm, angle 1°), with 0.05 mm sample thickness, at 20 ± 0.1 °C (in triplicate). To determine linear viscoelastic region of the samples oscillatory measurements were carried out (amplitude sweep), at constant frequency of 1 Hz and amplitude sweep ramp from 0.5 to 100 Pa. Once this region was established, the frequency sweep was performed within the linear region from 0.1 to 10 Hz at constant shear stress (1 Pa).

In vivo skin hydration/efficacy study

In vivo assessment of cream samples' hydration potential was conducted by non-invasive bioengineering techniques. To assess efficacy of formulated creams *stratum corneum* hydration (SCH) and transepidermal water loss (TEWL) were measured. A panel of 25 healthy volunteers (average age 26 ± 3.1) without the history of dermatological disease participated in the 5 h short-term study. Before the study, volunteers were thoroughly informed about possible treatment effects, as well as expected conduct during the experiment. Signed written consents were obtained in accordance with the Helsinki Declaration and local Ethical Committee. Volunteers were obliged to refrain from using topical products 2 days prior to and throughout the experiment.

Measurements were conducted under controlled temperature (22 ± 1 °C) and humidity ($35 \pm 5\%$) conditions, after 30 min acclimatization period. All measurements were conducted on flexor aspects of forearms, at 4×4 cm² application sites. A plastic template was applied to delimit test areas which were placed 1–2 cm apart and 6 cm away from the wrist and elbow. A calibrated Cutometer[®] MPA580 (with integrated Corneometer[®]CM825) and Tewameter[®]TM210 (Courage + Khazaka, Germany) were used for measurement of SCH and TEWL. Skin hydration and TEWL measurements were conducted at baseline (prior to), 1, 2, 3, and 5 h after sample application in the short-term study. All parameters were measured according to relevant guidelines [21].

Statistical analysis

Whenever applicable, obtained results were expressed as mean \pm SD. Comparison of all raw data involved a normality and equal variance test. When equal variance and normality were found, a parametric one-way ANOVA was used. Post hoc Tukey test was applied, where appropriate.

All statistical analyses were performed using SigmaStat (Version 3.1, Virginia, USA) and significance levels were $p < 0.05$.

Results and discussion

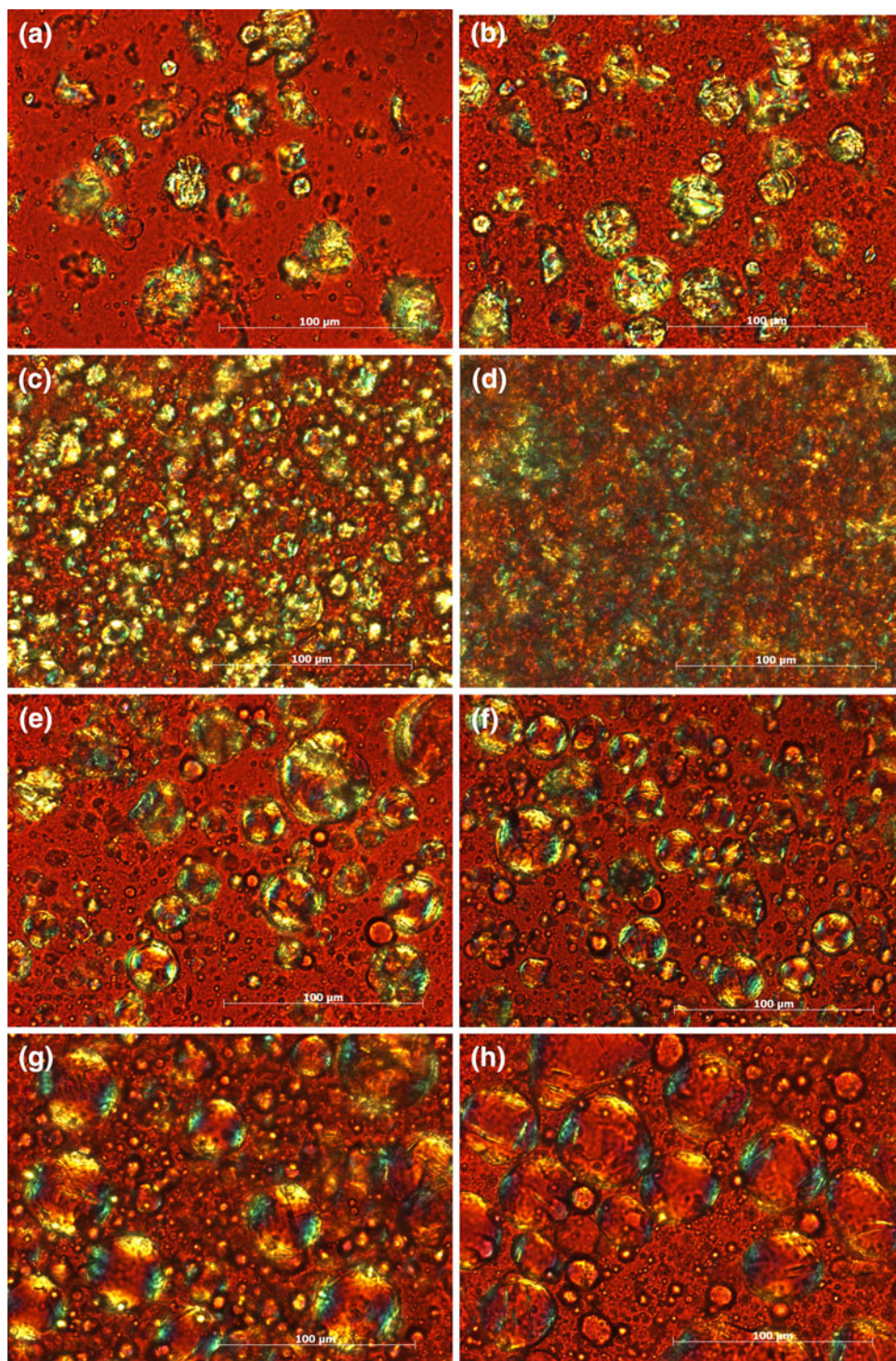
Complete structuring of emulsions stabilized with non-ionic surfactants is usually accomplished within several weeks [22]. Although the previous statement is more connected to the behavior of polyoxyethoxylated non-ionic surfactants, to investigate the stabilization potential of long-chain APG emulsifier properly performing the preliminary screening of the obtained mesophases, we took the polarization micrographs on two occasions, 7 and 30 days after the samples preparation. In addition, it was of interest to evaluate the influence of emulsifier concentration within the binary systems as well as the oil concentration increase in ternary systems on the specific phase behavior of the APG emulsifier (Fig. 1). The idea was to recognize the most promising concentration range of both for optimal emulsion formulation development. Furthermore, the influence of different oil phases (oils of different polarity, chemical composition, and origin) on specific structures' formation was evaluated (Fig. 2).

Anisotropic structures, defined as distorted Maltese crosses [8, 23], visible at polarization micrographs (Figs. 1a–h, 2a–c), as well as birefringence at the oil droplets border indicate the presence of lamellar structures probably of both types, i.e., lamellar liquid-crystalline and α -crystalline gel phases.

In binary systems, the increase of emulsifier concentration (Fig. 1a–d) led to the increase in both number and size of anisotropic structures. Careful observation of recorded binary systems' micrographs revealed the presence of emulsifier crystals, expected in binary systems due to the excess of the emulsifier and the absence of oil phase. Polarization micrographs of ternary systems with increased oil concentration (Fig. 1e–h) showed anisotropic droplets (“onion rings”) being more numerous and larger with the oil percentage variation from 5 to 20%. Further increase of the oil phase (sample T30mc—Fig. 1h) did not alter appearance of polarization micrographs when compared with sample T20mc (Fig. 1g).

With selected range of oils the investigated mixed APG emulsifier formed soft creams stabilized with lamellar phase as well, probably of both types (Fig. 2a–c). With oils of medium polarity (avocado oil and medium-chain triglycerides, Fig. 2a, b, respectively) distinct lamellar phase formation is characterized by numerous distorted Maltese crosses when observed between crossed polars. However, it is clear from the Fig. 2c that non-polar liquid paraffin oil,

Fig. 1 Polarization micrographs of $C_{20/22}$ APG mixed emulsifier binary systems (a–d): **a** B1, **b** B2, **c** B4, **d** B6 and ternary systems with medium-chain triglycerides (e–h): **e** T5mc, **f** T10mc, **g** T20mc, and **h** T30mc



although formed a stable cream with small oil droplets, reduced the specific birefringence.

Polarization microscopy was used to detect and confirm the presence of specific lamellar mesophases as the first and usual step in this type of studies [15], but for the more reliable insight and identification of the particular phases within the system, the assessment of

WAXD and SAXD profiles was performed. It is a well known fact that diffraction characteristics of hydrocarbon chains in α -crystalline gel phase ($L\beta$), namely the presence of a sharp peak that appears at 0.41–0.42 nm with the additional patterns within the small-angle region, imply presence of the lamellar liquid-crystalline phase [23].

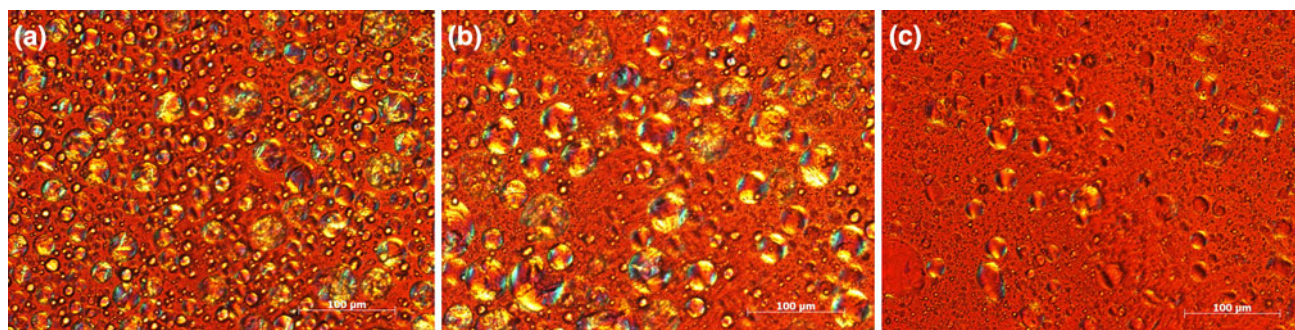


Fig. 2 Polarization micrographs of ternary systems with: **a** avocado oil—T20ao, **b** medium-chain triglycerides—T20mc, and **c** liquid paraffin—T20lp

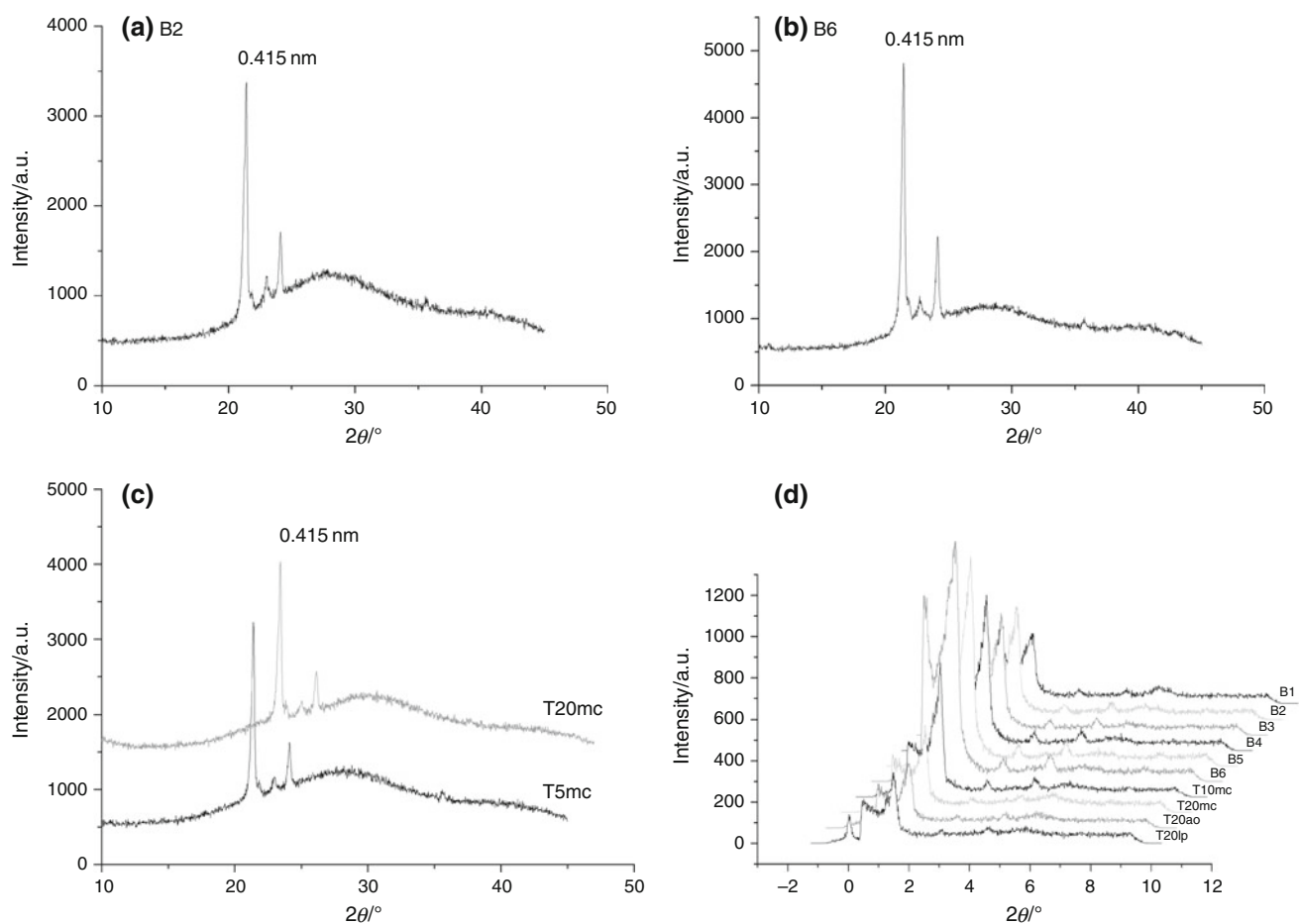


Fig. 3 WAXD profiles of binary systems: **a** B2, **b** B6, **c** ternary systems: T5mc and T20mc, and **d** SAXD patterns of investigated binary and selected ternary systems

Therefore, the obtained WAXD patterns with a single sharp reflection at 0.415 nm (Fig. 3) confirm the presence of α -crystalline gel phase both in binary and ternary systems. As expected, the intensity of interference increases with the increase of emulsifier content in binary systems (Fig. 3a, b). However, in ternary systems decrease in intensity is noticeable with increase of oil concentration (Fig. 3c).

In addition, in all samples there were signs of diffuse halo, in the part of the diffraction pattern next to the single peak, at 0.45 nm. Therefore, alongside the dominant lamellar α -crystalline phase ($L\beta$) WAXD results indicate also the presence of the lamellar liquid-crystalline phase ($L\alpha$).

WAXD findings were supported with the SAXD ones (Fig. 3d), confirming in that way the existence of a strongly

ordered structure containing lamellae with well-defined repeated distance, i.e., sharp reflections in the ratio $d:d/2:d/3$, the characteristic of lamellar liquid-crystalline phase.

As previously mentioned, DSC measurements enable recording of mass transfer phenomena during melting within an emulsion submitted to steady heating [11]. Melting points and enthalpy changes are assessed in order to detect the type of obtained mesophase(s) and to compare the phase transitions occurring within the investigated samples. In this term, for binary systems the influence of emulsifier concentration was investigated, i.e., it was of interest to recognize the type of mesophase reached with predetermined emulsifier concentration range which could fit to the desirable semisolid consistency of definitive emulsion formulations. On the other side, for ternary systems the aim of DSC study was to evaluate the influence of oil phase type and its concentration on their colloidal structure.

The DSC thermal behavior of the pure emulsifier and binary systems is shown in Fig. 4a. The pure emulsifier was characterized by three distinct peaks with total enthalpies of 787.2, 1608.1, and 205.4 mJ/mg, respectively. Melting points for arachidyl and behenyl alcohol are shown to be in the range 64–66 °C, i.e., 68–72 °C [24, 25].

Broad second endothermic peak at 64–71 °C could therefore correspond to the free alcohols melting, whereas the third one, smaller and sharper, could represent the melting of the alkyl polyglucoside blend, as a surfactants' part of the mixed emulsifier. However, the first peak could represent the free arachidyl and behenyl alcohols β - α transition at 42.5 °C [14].

On the other hand, binary systems are represented by only one broad endothermic peak, showing a distinct shift toward both higher ΔH (Table 3) and higher melting temperatures. According to Savic et al. [8], structures formed as the result of the water incorporation between the lipid lamellae (bilayers) having the complex composition, could modify the phase transition in such manner. The considerable activation energy required for melting of binary systems considered in conjunction with the results of polarization microscopy, WAXD, and SAXD measurements may be interpreted by the formation of complex lamellar phase consisted of both the liquid-crystalline and gel crystalline type mesophases. In addition, thermograms of binary systems (B1–B5) where the absence of β - α transition is noticeable indicate that the alkyl chains of fatty alcohols in these binary mixtures are in α -crystalline form at room temperature [14]. DSC results implied that

Fig. 4 DSC thermograms of **a** pure emulsifier and binary systems, **b** ternary systems with increased oil concentration, and **c** ternary systems with different oil phases, **d** schematic presentation of assumed lamellar structure organization of $C_{20/22}$ APG-mixed emulsifier systems

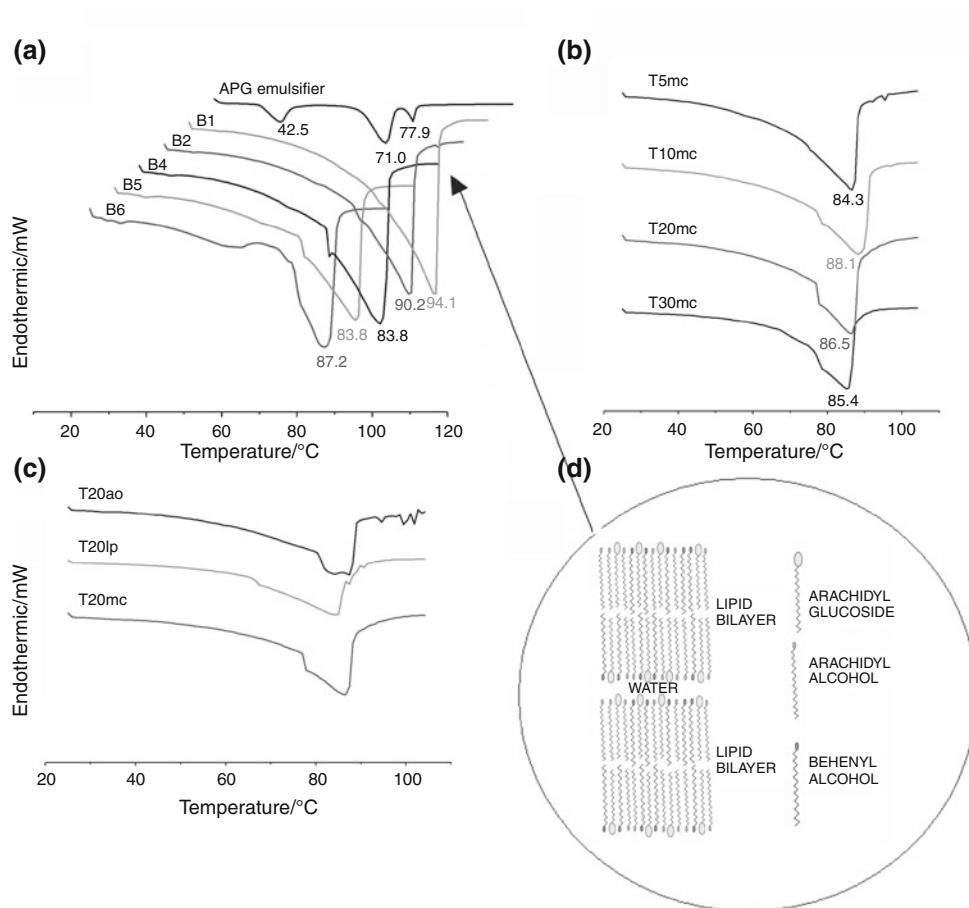


Table 3 DSC integration data—melting enthalpies/mJmg⁻¹, expressed as mean ± standard deviation

Sample	$\Delta H/\text{mJ}/\text{mg} \pm \text{Sd}$
B1	2100.7 ± 57.5
B2	1986.1 ± 23.7
B3	1946.8 ± 21.8
B4	1907.7 ± 1.7
B5	1733.8 ± 8.5
B6	1352.4 ± 29.3
T5mc	1790.6 ± 32.9
T10mc	1785.3 ± 13.2
T20mc	1482.4 ± 43.8
T30mc	1292.7 ± 8.3
T20ao	1504.3 ± 17.4
T20lp	1512.2 ± 52.2

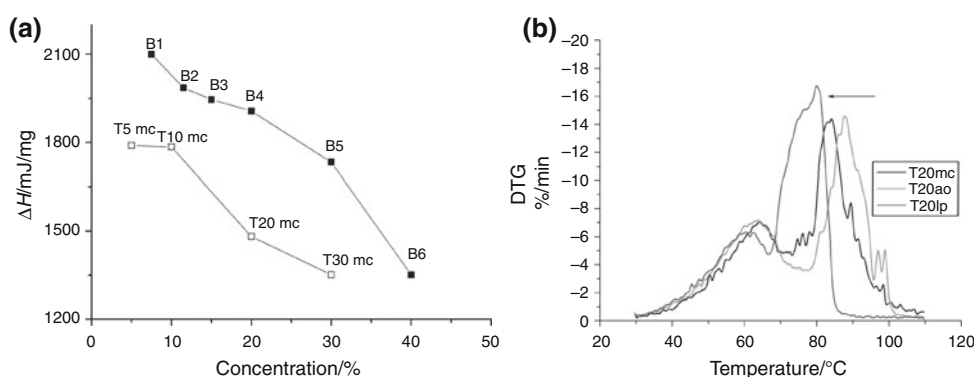
the melting (peak) temperatures (Fig. 4a) and ΔH (Fig. 5a) increased with higher water content (decrease of emulsifier concentration). Taking into account previously published data [8], consideration of the lamellar structures within these systems undoubtedly suggests that alkyl glucoside units are probably interpositioned among the fatty alcohol molecules as it is assumed in schematic presentation in Fig. 4d. Therefore, the possible explanation for the observed DSC behavior could be that with higher water content there is an increase in swelling of the α -crystals of alcohols due to the hydration of glucoside head groups which are oriented and infiltrated into the interlamellar water layers. At the same time the alkyl glucoside unit gradually dissolves at increasing water content. This stands in agreement with literature data on higher melting points of hydrated α -phase versus dehydrated one [26].

DSC curve of the sample with 5% of oil phase (T5mc, Fig. 4b) quite resembles the binary system (B2) DSC curve. Addition of medium-chain triglycerides lowered the total enthalpy of the system transition, which gradually decreases with the increase of oil concentration within the emulsion (Figs. 4b, 5a). Namely, comparing to the corresponding binary system, the endothermic peak recorded in

all ternary systems is narrower with a distinct shift towards lower melting temperatures with emersion of the peak's shoulder detected also at lower temperatures. Besides, all observed alterations are more pronounced with the increase of oil concentration. A possible explanation for this finding lies in the insertion of medium alkyl chains from the oil constituent into the lipid bilayers which can disrupt close packing of the mixed APG emulsifier, thus affecting their swelling behavior and lamellar phase formation. Lamellar phase whose formation could be primarily altered in this manner is the hydrophilic lamellar gel, consisting of the part of APG units and part of both long-chain fatty alcohols. As a consequence, a part of the oily phase may be solubilised in this structure making the relatively rigid gel structure more fluid which results in the observed decrease in ΔH and peak temperatures.

Thermal behavior of ternary systems with oils of different polarity was subsequently assessed (Fig. 4c), and manifested as similar in the shape of DSC curves previously obtained for ternary systems with medium-chain triglycerides, with similar ΔH values (Table 3) and peak temperatures (82.5–85.9 °C). DSC curve of the sample T20lp with non-polar liquid paraffin differed from other curves, and was characterized by a very broad endothermic peak. This stands in agreement with previously discussed results of polarization microscopy and could be explained with the reduction of specific lamellar structure. Formation of lamellar structures depends on the ability of molecules to pack together closely and to interact with water. As liquid paraffin is composed of non-polar, medium-chain alkanes (hydrocarbons), it could be presumed that the insertion of hydrocarbons in long-chain alcohols' lipid bilayers strongly disrupts lamellar structure. This may be partially due to the length of liquid paraffin hydrocarbon chains which are almost twice as shorter than the investigated long-chain APG emulsifier. Comparison of results obtained for oils of medium polarity (medium-chain triglycerides and avocado oil) and for non-polar oil (liquid paraffin) indicates that the capability of investigated long-chain APG emulsifier to stabilize emulsion systems by

Fig. 5 **a** Plot of the melting enthalpy (ΔH) versus percentage of the APG emulsifier (solid squares) and percentage of medium-chain triglyceride oil (open squares) and **b** derivative TG profiles of ternary systems with medium-chain triglycerides (T20mc), avocado oil (T20ao) and liquid paraffin (T20lp)



lamellar phase formation is reduced in the non-polar medium.

Obtained DSC results are in accordance with the conducted thermogravimetric measurements, performed in a trial to investigate the mode of water distribution within the system more precisely. Direct assessment of TG profiles enabled insight into samples' partial weight losses over different temperature ranges; whereas the comparison of first derivative TG curves (DTG profiles) indirectly pointed to the water evaporation rates from different systems.

Since there are no other volatile (non-aqueous) components in all investigated samples, the recorded losses inevitably correspond to the water in the system, and the calculation is performed relative to total formulation water content (Table 4). Obtained TG findings imply that the water in all binary and ternary systems is predominantly incorporated as interlamellarly fixed (so-called depot) water, and hence mainly evaporated at the third temperature range (70–110 °C) (Table 4). This probably occurs upon the subsequent disruption (dehydration and melting) of the lamellar phases (lipid lamellae) of different types: (1) more fluid liquid-crystalline lamellae built mostly from APG surfactant units; (2) more rigid hydrophilic lamellar gel randomly oriented through the continual phase of the ternary systems, consisting of the part of APG units and part of both long-chain fatty alcohols, and (3) rigid lipophilic gel with the small part of dispersed oil within, which mostly contains semi-hydrates of arachidyl and behenyl alcohols. That means that beside highly hydrated APG units of the mixed emulsifier, behenyl, and arachidyl alcohols being in excess may be also responsible for binding a part of the water, appearing in that way as some form of fixed water (so-called secondary water) [20, 27].

Certainly, it could be seen that in binary systems percentage of water evaporation during the third stage (temperature range 70–110 °C) gradually increased from 60.97% in binary system B1 to 68.15% in B6 (Table 4). As expected, with the increase of emulsifier content in binary systems the water is interlamellarly fixed to a greater extent. However, in the ternary systems, the increase of oil concentration led to decrease of water evaporation in the third temperature stage. These results stand in an agreement with WAXD and DSC measurements, supporting the previous assumption that with increased oil concentration lamellar phase formation is reduced.

When considering the samples with different oil phases (Table 4), percentages of water evaporation during the third stage were from 48.13% (in sample with liquid paraffin, T20lp) to the 63.48% (in sample with avocado oil, T20ao) suggesting that more than one half of water within the system is somehow entrapped (e.g., as interlamellarly fixed—'depot' water). Sample with liquid paraffin had the highest water evaporation rates during the first (30–50 °C) and the second (50–70 °C) temperature range, and as previously mentioned the lowest during the third one, pointing to the low compatibility of the long-chain APG mixed emulsifier with non-polar oil phase, potentially indicating not satisfying long-term physical stability of the system.

Further examination of DTG curves shows that all samples except T20lp sample exhibited similar behavior concerning the evaporation rate. DTG curves for samples T20mc and T20ao mostly overlap until 70 °C (Fig. 5b) and afterwards, with clear similarity in water evaporation mode (Tables 4, 5). T20lp curve (Fig. 5b, pointed with an arrow) is shifted toward lower temperatures and the evaporation is

Table 4 Percentage water loss values over the specified temperature ranges for binary systems, ternary samples with different amount of oil and ternary samples with different oils; results are presented as mean \pm standard deviation

Sample	Water loss 30–50 °C/%	Water loss 50–70 °C/%	Water loss 70–110 °C/%
B1	5.77 \pm 1.40	32.36 \pm 0.91	60.56 \pm 0.72
B2	5.90 \pm 0.61	29.82 \pm 0.03	60.97 \pm 0.02
B3	5.87 \pm 2.11	28.27 \pm 0.21	62.24 \pm 0.10
B4	5.33 \pm 0.91	29.46 \pm 0.12	62.18 \pm 0.30
B5	8.48 \pm 0.76	24.32 \pm 0.41	66.15 \pm 0.03
B6	11.48 \pm 0.67	19.32 \pm 0.32	68.15 \pm 0.08
T5mc	4.89 \pm 0.80	24.38 \pm 0.03	66.21 \pm 1.77
T10mc	6.04 \pm 0.23	26.30 \pm 1.23	63.49 \pm 0.72
T20mc	5.96 \pm 0.97	29.17 \pm 0.78	58.97 \pm 1.02
T30mc	7.84 \pm 1.12	26.69 \pm 1.23	54.63 \pm 0.86
T20ao	5.59 \pm 2.55	26.30 \pm 0.91	63.46 \pm 0.09
T20lp	9.28 \pm 1.13	35.00 \pm 0.08	48.13 \pm 1.23

Percentage water loss was calculated relative to total water content

Table 5 Temperature ranges for the highest evaporation rates

Sample	Temperature range/°C
T20mc	78.7–96.9
T20ao	79.2–100
T20lp	66.8–84.4

the highest between 66.8 and 84.4 °C, addressing the aforementioned less rigid stabilization lamellar phase of gel type and potential problems with the system instability.

For more comprehensive investigation of emulsifiers' ability to stabilize emulsions, certain rheological measurements were conducted. Flow parameters obtained by continual and/or oscillatory rheological measurements provide information regarding the systems' colloidal structure and physical stability, important from both fundamental and applied points of view [28, 29]. In addition, flow and viscoelastic properties are known to exhibit influence on drug/cosmetic actives release from semisolids [30].

As confirmed by the appearance of hysteresis loop area in the plot of shear stress versus shear rate (Fig. 6), all the samples exhibited shear-thinning, time-dependant (thixotropic) behavior. This reversible and time-dependent rheological manifestation of flow-induced structural changes is considered desirable for all topically applied preparations [29]. Flow curves show, as seen in Fig. 6 that in binary systems (Fig. 6a) thixotropy was more pronounced in samples with higher emulsifier content, and in ternary systems (Fig. 6b) in samples with higher oil concentration.

Gradual increase of hysteresis area and maximal apparent viscosity values of binary (Fig. 6a; Table 6) and ternary (Fig. 6b) systems confirms thickening as the result of higher emulsifier and oil concentration. In fact, the thickening phenomena is mostly attributed to the lamellar phase formation—liquid-crystalline lamellae surrounding the dispersed oil droplets and both types of lamellar gel spreading throughout the continual phase. Under shear the orientation of the lamellae is changing and depending on the domain–domain interactions external stress defines the viscosity of the system [31]. Moreover, such rheological

Fig. 6 Flow curves of **a** binary systems, **b** ternary systems with increasing oil concentration, **c** ternary systems with different oil phase component, and **d** elastic (G' —solid line) and viscous (G'' —dotted line) modulus as a function of frequency for ternary systems with different oil phase component

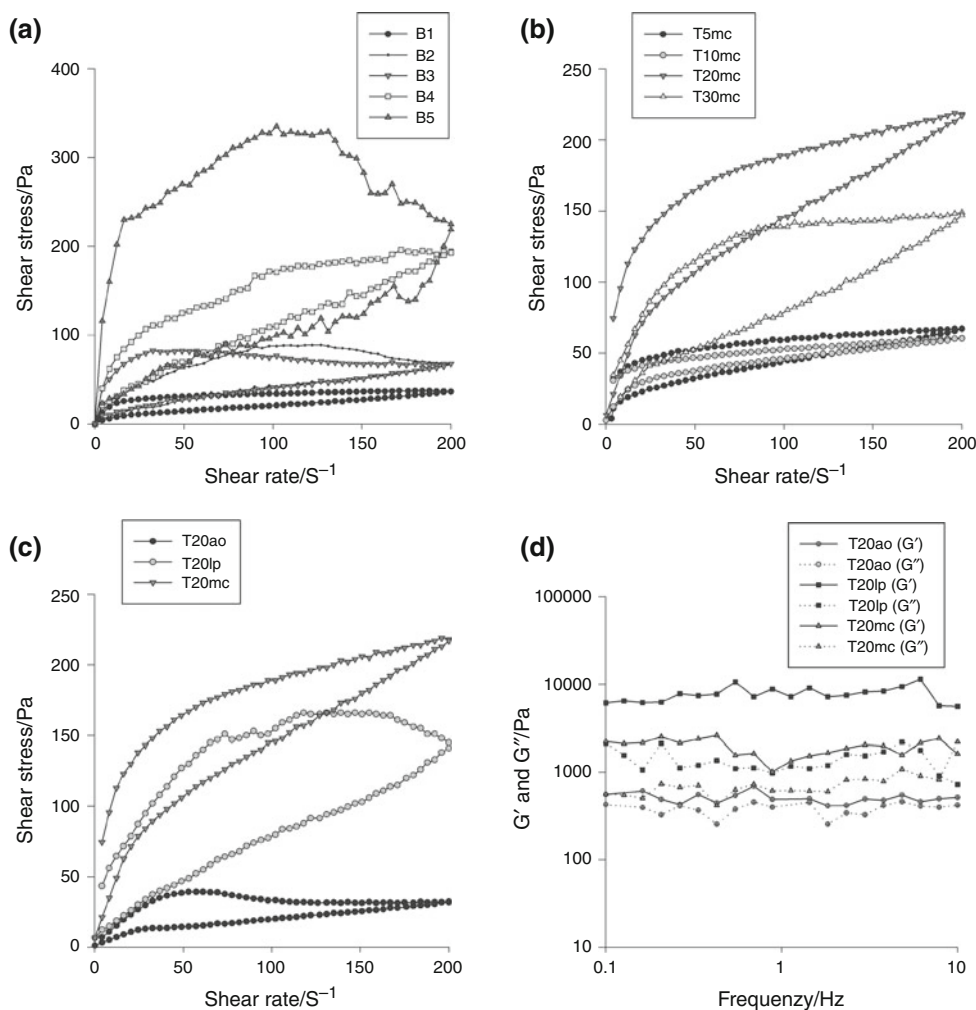


Table 6 Hysteresis area and maximal apparent viscosity values for binary and ternary systems

Sample	η_{\max} (4.08/s)	Hysteresis area/Pa/s
B1	2.97 ± 0.04	2259 ± 12
B2	3.18 ± 0.02	6085 ± 7
B3	9.75 ± 0.11	6422 ± 12
B4	9.80 ± 0.42	8637 ± 22
B5	28.41 ± 0.09	34698 ± 20
B6	214.12 ± 1.23	137391 ± 54
T20mc	18.30 ± 0.91	7714 ± 12
T20ao	1.73 ± 0.08	2322 ± 5
T20lp	10.60 ± 0.87	12239 ± 43

findings corresponding to the thermal analysis hints additionally prove the assumption on the synergism between the two main types of lamellar phases in this sort of the systems: the liquid-crystalline ($L\alpha$) and the gel crystalline ($L\beta$) one.

Flow behavior in steady state measurements and the appearance of rheological curves are often used for the prediction of behavior upon application. Figure 6b shows that the increase in oil phase from 5 to 20% has led to the thickening of the system (higher yield stress and hysteresis area). In sample T30mc the observed trend seems to be stopped, i.e., yield stress decreased while the hysteresis area increased. Topically applied preparations are expected to show certain resistance to the applied stress—manifested in rheology as yield stress [32]. Afterwards, the system starts to flow, practically is spread to the applied area and this is manifested as shear-thinning and thixotropic behavior, and ease of spreading could be quantified with hysteresis area value.

Obtained rheological curves show that the system with 30% of oil phase has smaller yield stress and bigger hysteresis area indicating that this system could be less physically stable and more difficult to apply than system with 20% of oil phase.

The emulsions with different oils, although containing the same percentage of oil phase, showed different rheological profiles in steady state measurements (Fig. 6c). Alongside with the viscosity of cream samples, hysteresis areas significantly differed (Table 6) indicating the alterations regarding the systems' structure. This is probably due to diverse packaging of their molecules into the liquid-crystalline or gel crystalline lamellae.

In addition, for the cream samples with different oils the linear viscoelastic region was determined and frequency sweep test was performed in order to avoid emulsion structure disturbance. Oscillatory measurements showed that storage modulus (G') had higher values in viscoelastic region than loss modulus (G'') for all examined samples

(Fig. 6d shows G' and G'' curves dependent on applied frequency for samples T20mc, T20ao, and T20lp), implying more pronounced elastic over viscous component—one of the general characteristics of lamellar phase.

Previous results confirmed the presence of the lamellar phase for the sample T20ao, yet, results obtained by oscillatory measurements were not as expected: with one magnitude order differences between G' and G'' . Although G' values were higher, they were of the same order of magnitude as G'' values. Nevertheless, this is in agreement with the findings of Siddig et al. [33] who showed that the discrepancy between G' and G'' could be small in lamellar phase and that the elastic properties although more pronounced could be at the same order of magnitude as viscous ones, especially at the higher frequency.

In addition, to investigate hydration potential of cream samples in the real-time conditions and complementary to previously conducted thermoanalytical analysis, in vivo study on the human volunteers was performed. Samples with medium-chain triglycerides (medium polarity oil), avocado oil (natural origin and medium polarity oil), and liquid paraffin (non-polar oil) were subjected in this study.

One hour after the sample application, with the exception of liquid paraffin containing sample, a certain decrease in skin hydration (SCH) was recorded (Fig. 7) without a change in transepidermal water loss (TEWL) values for any treated site. Usually, 1 h short-term studies show increase in SCH due to higher water content in SC as the result of creams' water liberation. Our results indicate that the amount of free—loosely bound water ready to evaporate from the skin shortly after the application and therefore capable to increase SCH in the short time, is negligible in samples with medium-chain triglycerides and avocado oil, which stands in agreement with TG analysis (Table 4) and percentage of water evaporation during the first stage

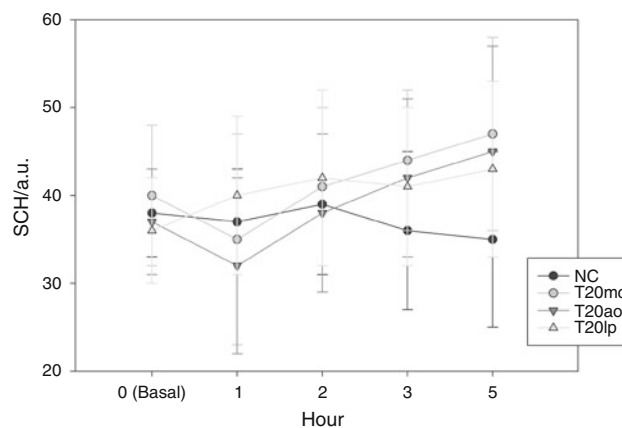


Fig. 7 Obtained stratum corneum hydration values (SCH in arbitrary units) for different time points measured after the application of investigated samples T20mc, T20ao, T20lp, and NC (non-treated control); presented as mean ± standard deviation

(temperature range 30–50 °C). As expected, 2 and 3 h after the samples' application SCH values gradually increased, while the final measurement (after 5 h) revealed a significant SCH increase in all treated sites (Fig. 7). Explanation for this prolonged moisturizing effect could be the gradual liberation of the interlamellar water, particularly from the samples T20mc and T20ao.

It is known that application of emulsions stabilized with commonly used nonionic surfactants (ethoxylated and propoxylated derivatives and polyol esters) increases the TEWL due to a change in the properties of lamellar lipids of SC intercellular matrix [34, 35]. However, during our 5 h study TEWL values were not significantly changed in any time point for any sample. The absence of TEWL change could be due to the similarity of samples' liquid-crystalline structure with the structure of physiological skin lipids. This confirms favorable safety profile of investigated APG emulsifier on one hand and on the other the presence of specific colloidal structure of APG stabilized vehicles.

Conclusions

Investigated long-chain APG emulsifier proved to have high potential in lamellar phase formation when it is used in reasonable concentration range. Obtained results showed that in systems stabilized with this mixed emulsifier synergism between the two main types of lamellar phases: the liquid-crystalline ($L\alpha$) and the gel crystalline ($L\beta$) one, exists. Formation of lamellar structures enabled for more than one half of water within the system to be somehow entrapped (e.g., as interlamellarly fixed—"depot" or "secondary" water fractions). Conducted investigation of hydration potential in real-time conditions provided valuable information on the investigated emulsion vehicles' moisturizing potential as well as their contribution to the skin barrier improvement. Therefore, it could be expected that emulsions based on this APG emulsifier could influence the delivery of active ingredients of both the lipophilic and hydrophilic type.

Studies related to the effect of the oil phase concentration and composition showed that the increase in oil phase content reduces lamellar phase formation. Although the investigated emulsifier showed a considerable potential for lamellar phase formation, our results indicate the importance of the oil phase selection. In that context, it was demonstrated that in the presence of liquid paraffin, as a non-polar oil, the stability of the obtained mesophases appears to be compromised, implying a potential compatibility concern between the investigated long-chain APG mixed emulsifier with a non-polar oil phase.

Thermoanalytical methods employed in this study (DSC and TG), performed to investigate mesomorphic behavior of C_{20/22} APG-mixed emulsifier and to elaborate the mode of water distribution within the selected systems enabled previous conclusions to be made. Other techniques commonly employed in the characterization of investigated systems such as microscopy, rheology, and X-ray diffraction methods confirmed the results obtained by thermoanalytical methods, proving the possibility for thermal methods to be used more frequently in the characterization of both the novel raw materials useful for emulsion systems stabilization as well as the complex emulsion systems per se.

Acknowledgements The authors would like to acknowledge the financial support from the Ministry of Science and Technological Development, Republic of Serbia (Project number TR34031).

References

1. Stubenrauch C. Sugar surfactants—aggregation, interfacial and adsorption phenomena. *Cur Opin Colloid Interf Sci.* 2001;6: 160–70.
2. Savic S, Weber C, Tamburic S, Savic M, Müller-Goyman C. Topical vehicles based on natural surfactant/fatty alcohols mixed emulsifier: the influence of two polyols on the colloidal structure and in vitro/in vivo skin performance. *J Pharm Sci.* 2009;98: 2073–90.
3. Savic S, Lukic M, Jaksic I, Reichl S, Tamburic S, Müller-Goyman C. An alkyl polyglucoside-mixed emulsifier as stabilizer of emulsion systems: the influence of colloidal structure on emulsion hydration potential. *J Colloid Interf Sci.* 2011;358:182–91.
4. Tadros TF. Applied surfactants—principles and applications. Weinheim: Wiley VHC; 2005.
5. Mehling A, Hensen H. Comparative studies on the irritation potential of surfactants. *Exog Dermatol.* 2004;3:191–200.
6. Lodén M. The clinical benefit of moisturizers. *J Eur Acad Dermatol Venerol.* 2005;19:672–88.
7. Wang X, Ujihara M, Imae T, Ishikubo A, Sugiyama Y, Okamoto T. Characterization of mimetic lipid mixtures of stratum corneum. *Colloid Surf B.* 2010;78:92–100.
8. Savic S, Vuleta G, Daniels R, Müller-Goyman C. Colloidal microstructure of binary systems and model creams stabilized with alylpolyglucoside non-ionic emulsifier. *Colloid Polym Sci.* 2005;283:439–51.
9. Makai M, Csányi E, Németh Zs, Pálkás J, Erős I. Structure and drug release of lamellar liquid crystals containing glycerol. *Int J Pharm.* 2003;256:95–107.
10. Savic S, Savic M, Tamburic S, Vuleta G, Vesic S, Müller-Goyman C. An alkylpolyglucoside surfactant as a prospective pharmaceutical excipient for topical formulations: the influence of oil polarity on the colloidal structure and hydrocortisone in vivo/in vitro permeation. *Eur J Pharm Sci.* 2007;30:441–50.
11. Clause D. Differential thermal analysis, differential scanning calorimetry, and emulsions. *J Thermal Anal Calorim.* 2010;101: 1071–7.
12. Clause D, Gomez F, Pezron I, Komunjer L, Dalmazone C. Morphology characterization of emulsion by differential scanning calorimetry. *Adv Colloid Interf Sci.* 2005;117:59–74.

13. Schwarz E, Pfeffer S. Use of subambient DSC for liquid and semisolid dosage forms Pharmaceutical product development and quality control. *J Thermal Anal Calorim.* 1997;48:557–67.
14. Goetz R, El-Aasser M. Dilute phase behavior of cetyl alcohol, sodium lauryl sulfate, and water. *Langmuir.* 1990;6:132–6.
15. Zetzl A, Ollivon M, Marangoni A. A coupled differential scanning calorimetry and X-ray study of the mesomorphic phases of monostearin and stearic acid in water. *Cryst Growth Des.* 2009;9:3928–33.
16. Kalnin D, Schafer O, Amenitsch H, Ollivon M. Fat crystallization in emulsion: influence of emulsifier concentration on triacylglycerol crystal growth and polymorphism. *Cryst Growth Des.* 2004;4:1283–93.
17. Awad TS, Helgason T, Weiss J, Decker EA, McClements DJ. Effect of omega-3 fatty acids on crystallization, polymorphic transformation and stability of tripalmitin solid lipid nanoparticle suspensions. *Cryst Growth Des.* 2009;9:3405–11.
18. Csizmazia E, Budai-Szűcs M, Erős I, Makai Z, Szabó-Révész P, Varju G, Csányi E. Thermoanalytical method for predicting the hydration effect permanency of dermal semisolid preparations. *J Thermal Anal Calorim.* 2010;101:313–6.
19. Kónya M, Sorrenti M, Ferrari F, Rossi S, Csóka I, Caramella C, Bettinetti G, Erős I. Study of the microstructure of oil/water creams with thermal and rheological methods. *J Thermal Anal Calorim.* 2003;73:623–32.
20. Peramal VL, Tamburic S, Craig DQM. Characterization of the variation in the physical properties of commercial creams using thermogravimetric analysis and rheology. *Int J Pharm.* 1997;155:91–8.
21. Berardesca E. EEMCO guidance for the assessment of stratum corneum hydration: electrical methods. *Skin Res Tech.* 1997;3:126–32.
22. Lashmar UT, Richardson JP, Erbod A. Correlation of physical parameters of an oil in water emulsion with manufacturing procedures and stability. *Int J Pharm.* 1995;125:315–25.
23. Fairhurst CE, Fuller S, Graz J, Holmes MC. Lyotropic surfactant liquid crystals. In: Demus D, Goodby J, Gray GW, Spiess HW, Vill V, editors. *Handbook of liquid crystals*, vol 3rd. Weinheim: Wiley VCH; 1998. p. 341–92.
24. Material Safety Data Sheet. 2009. http://www.chemblink.com/MSDS/MSDSFiles/629-96-9_SigmaAldrich.pdf. Accessed 05 Aug 2011.
25. Material Safety Data Sheet. 2008. http://www.chemblink.com/MSDS/MSDSFiles/661-19-8_SigmaAldrich.pdf. Accessed 05 Aug 2011.
26. Ecclestone GM. Functions of mixed emulsifiers and emulsifying waxes in dermatological lotions and creams. *Colloid Surf A.* 1997;123–124:169–82.
27. Junginger HE. Pharmaceutical emulsions and creams. In: Sjöblom J, editor. *Emulsions—a fundamental and practical approach*. Dordrecht: Kluwer Academic Publishers; 1992. p. 189–205.
28. Tadros ThF. Fundamental principles of emulsion rheology and their applications. *Colloids Surfaces A.* 1994;91:39–55.
29. Tadros T. Application of rheology for assessment and prediction of the long-term physical stability of emulsions. *Adv Colloid Interf Sci.* 2004;108–109:227–58.
30. Dragicevic-Curic N, Winter S, Stupar M, Milic J, Krajisnik D, Gitter B, Fahr A. Temoporfin-loaded liposomal gels: viscoelastic properties and in vitro skin penetration. *Int J Pharm.* 2009;373:77–84.
31. Nemeth Z, Halasz L, Palinkas J, Bota A, Horanyi T. Rheological behaviour of a lamellar liquid crystalline surfactant-water system. *Colloid Surf A.* 1998;145:107–19.
32. Barnes HA. The yield stress—a review or ‘panta rei’—everything flows. *J Non-Newtonian Fluid Mech.* 1999;81:133–78.
33. Siddig MA, Radiman S, Jan LS, Muniandy SV. Rheological behaviors of the hexagonal and lamellar phases of glucopone (APG) surfactant. *Colloid Surf A.* 2006;276:15–21.
34. Bárány E, Lindberg M, Lodén M. Unexpected skin barrier influence from nonionic emulsifiers. *Int J Pharm.* 2000;195:189–201.
35. Idson B. Effect of emulsifiers on skin. *Cosmet Toiletries.* 1991;106:43–51.